SUBBAND ACOUSTIC ECHO CANCELLATION WITH CASCADED POWER SYMMETRIC IIR FILTER BANKS AND CONTINUITY CONSTRAINED ADAPTIVE ALGORITHMS

Oğuz Tanrıkulu and Anthony G. Constantinides

Signal Processing and Digital Systems Section,
Department of Electrical and Electronic Engineering,
Imperial College of Science, Technology and Medicine, London SW7 2BT, UK.
o.tanrikulu@ic.ac.uk

ABSTRACT

For highly selective filter-banks the aliasing in subband acoustic echo cancellers (AEC) is confined into very narrow spectral regions. Therefore, narrowband notch filters were introduced into the analysis-banks in order to attenuate the aliasing prior to echo cancellation. Two contributions are presented in this paper. Firstly, it is shown that the notch filtering operation can be implicitly performed by using Cascaded Power Symmetric IIR (PS-IIR) filter-banks. Secondly, the adaptive algorithms running in neighbouring subbands must be coupled via continuity constraints. Therefore the well-known NLMS algorithm is modified and the Continuity Constrained NLMS (CC-NLMS) algorithm is proposed. The simulation results confirm the attenuation of the aliased components.

1. INTRODUCTION

The primary advantage of subband AEC is the reduced computational complexity due to processing at reduced rates [1, 4]. Furthermore, practice has shown that the convergence is generally faster compared to full-band processing when NLMS like adaptive algorithms are used. This is usually ascribed to the possible decrease in the eigenvalue spread of the loudspeaker signal in each subband [2].

The limitations associated with subband AEC are the aliasing of neighbouring subband signals that impinge upon the echo cancellation performance and the delay introduced due to Multi-Rate Analysis Banks (MRABs) and Multi-Rate Synthesis Banks (MRSBs).

In [4], it is shown there that if highly selective filter banks are used, then aliasing is confined to narrow regions in the spectrum. Highly selective FIR filter banks are not practical since the increase in the computational complexity and delay may not be affordable. On the other hand, highly selective PS-IIR filter banks are easy to implement. However, two points remain. Firstly, aliasing occurs in the form of coherent spectral components around subband division frequencies. These are usually perceptually disturbing.

AN EXTENDED VERSION OF THIS PAPER IS SUBMITTED TO THE IEEE TRANS. ON SIG. PROC. AS A SPECIAL ISSUE ARTICLE ON "THEORY AND APPLICATIONS OF FILTER BANKS AND WAVELETS".

Secondly, the phase distortion on the reconstructed near-end speech is significant around subband edges. Therefore, notch filters have been used in [3, 4] to deal with both problems.

2. POWER SYMMETRIC IIR FILTER BANKS AND NOTCH FILTERING

A PS-IIR filter has the transfer function

$$H_0(z) = \frac{A_0(z^2) + z^{-1}A_1(z^2)}{2} \tag{1}$$

where

$$A_i(z^2) = \prod_{j=0}^{P_i-1} \frac{\alpha_{i,j} + z^{-2}}{1 + \alpha_{i,j}z^{-2}}, \quad i = 0, 1 \tag{2}$$

are cascaded second-order all-pass stages and $\alpha_{i,j}$ are the real all-pass coefficients. Highly selective low-pass filters can be designed by minimising the stop-band energy over a dense grid [7].

When $G_0(z) = 2H_0(z)$, and $G_1(z) = -2H_0(-z)$ for aliasing cancellation [6], the input-output transfer function of a cascaded MRAB and MRSB is given by

$$T(z) = z^{-1}A_0(z^2)A_1(z^2) \tag{3}$$

Hence, there is no amplitude distortion since $A_0(z^2)$ and $A_1(z^2)$ are all-pass transfer functions. There is, however, phase distortion and it is most significant around $\theta = \pi/2$ [4]. In [4], Distributed Notch Filters (DNF) are inserted at the input of each MRAB in the binary-tree so that the spectral components at the subband edges are attenuated over a narrow bandwidth. The findings in the next section show that the notch filtering operation can be performed implicitly by modifying the PS-IIR filter banks.

3. CASCADED PS-IIR (CPS-IIR) FILTER BANKS AND IMPLICIT NOTCH FILTERING

Let $H_0(z)$ be a low-pass, PS-IIR filter. Then, p-fold CPS-IIR transfer function

$$H_0^p(z) = \frac{\left[A_0(z^2) + z^{-1}A_1(z^2)\right]^p}{2^p}, \quad p = 2, 3, 4, \ldots \tag{4}$$

is also a low-pass filter. The pass-band sensitivity of $H_0(z)$ is very low, and therefore $H_0^p(z)$ has an acceptable pass-band ripple for small values of p. Moreover, the stop-band attenuation is p times higher. An example is shown in Fig. 1 where the following parameters are used; for $H_0(z)$ $(P_0, P_1) = (2, 1)$ and the stop-band frequency is $\theta_s = 1.885$ *rads*. The amplitude characteristics of $H_0^2(z)$ is also presented. A PS-IIR filter, $\breve{H}_0(z)$, with amplitude response similar to $H_0^2(z)$ is also designed with $(P_0, P_1) = (3, 3)$ and $\theta_s = 1.885$ *rads*. The all-pass coefficients of $H_0(z)$ and $\breve{H}_0(z)$ are tabulated in Table 1. For simulation purposes, a *perfect reconstruction* FIR (PR-FIR) filter is also designed [6] and presented in Fig. 1.

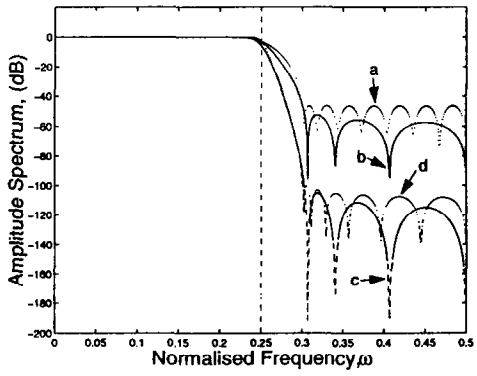

Figure 1: Amplitude spectra of various prototype filters; (a) PR-FIR, (b) $H_0(z)$ (PS-IIR), (c) $H_0^2(z)$ (CPS-IIR), (d) $\breve{H}_0(z)$ (PS-IIR).

All-pass coef.	$H_0(z)$	$\breve{H}_0(z)$
$\alpha_{0,0}$	0.778242	0.666472
$\alpha_{0,1}$	0.118008	0.293250
$\alpha_{0,2}$	-	0.037332
$\alpha_{1,0}$	0.408292	0.879585
$\alpha_{1,1}$	-	0.472206
$\alpha_{1,2}$	-	0.141475

Table 1: All-pass coefficients of $H_0(z)$ and $\breve{H}_0(z)$.

After expanding (4), we have

$$H_0^p(z) = \frac{1}{2^p}\sum_{i=0,i:even}^{p}\left(\frac{p}{p-i}\right)A_0^{p-i}A_1^i z^{-i} + \frac{1}{2^p}\sum_{i=0,i:odd}^{p}\left(\frac{p}{p-i}\right)A_0^{p-i}A_1^i z^{-i} \quad (5)$$

where we denote $A_0(z^2)$ by A_0 and $A_1(z^2)$ by A_1 for convenience, and $\binom{n}{k} \triangleq \frac{n!}{k!(n-k)!}$

Remark 1 (Polyphase structure) *Assume that p is even, then we have from* (5)

$$H_0^p(z) = \frac{\tilde{A}_0(z^2) + z^{-1}\tilde{A}_1(z^2)}{2} \quad (6)$$

where

$$\tilde{A}_0(z^2) \triangleq \frac{1}{2^{p-1}}\sum_{i=0}^{p/2}\left(\frac{p}{p-2i}\right)A_0^{p-2i}A_1^{2i}z^{-2i} \quad (7)$$

$$\tilde{A}_1(z^2) \triangleq \frac{1}{2^{p-1}}\sum_{i=0}^{p/2-1}\left(\frac{p}{p-2i-1}\right)A_0^{p-2i-1}A_1^{2i+1}z^{-2i} \quad (8)$$

and therefore CPS-IIR filter-banks can be implemented in polyphase form.

We also have the following theorem for the cascaded MRAB and MRSB of the CPS-IIR filter banks.

Theorem 1 *Consider the general CPS-IIR filter in* (4) *and let p be even with the analysis bank filters defined as $H_0^p(z)$ and $H_0^p(-z)$. Let the synthesis bank filters be $G_0(z) = 2H_0^p(z)$, and $G_1(z) = -2H_0^p(-z)$. Then,*

(i) the transfer function of the cascaded MRAB and MRSB is given by

$$\tilde{T}(z) = H_0^{2p}(z) - H_0^{2p}(-z) = z^{-1}\tilde{A}_0(z^2)\tilde{A}_1(z^2) \quad (9)$$

(ii) at $\theta = \pi/2$, if $p/2$ is odd, we have

$$\tilde{A}_0(z^2)\big|_{z=e^{j\pi/2}} = 0 \quad (10)$$

and if $p/2$ is even, we have

$$\tilde{A}_1(z^2)\big|_{z=e^{j\pi/2}} = 0 \quad (11)$$

Therefore, $\tilde{T}(\pi/2) = 0$, for all even p. In other words, there is a notch at the output of the cascaded MRAB and MRSB at $\theta = \pi/2$.

The proof is in [5] where the bandwidth of the notch in relation to the all-pass coefficients of the prototype low-pass PS-IIR filter, $H_0(z)$, is also given.

4. GENERIC TWO-BAND AEC UNIT

So far we have considered the cascaded MRAB and MRSB of CPS-IIR filter banks. In this section, we obtain the conditions such that the aliasing at the output of a generic two-band AEC unit is attenuated by an implicit notch filtering operation.

Let us make the following definitions. $X(z)$ is the loudspeaker signal that contains the far-end speech. $S(z)$ represents the acoustic echo path which is assumed to be linear and time-invariant [1]. $M(z) = S(z)X(z)$ is the acoustic echo and $E(z)$ is the full-band residual echo signal. $\mathbf{C}(z)$ is the 2×2 predictor matrix whose off-diagonal terms represent the cross-channel predictors [1, 4]. Define

$$\mathbf{x}(z) \triangleq [X(z)\ X(-z)]^T \quad (12)$$

$$\mathbf{S}(z) \triangleq \begin{bmatrix} S(z) & 0 \\ 0 & S(-z) \end{bmatrix} \quad \mathbf{H}(z) \triangleq \begin{bmatrix} H_0^p(z) & H_0^p(-z) \\ H_0^p(-z) & H_0^p(z) \end{bmatrix} \quad (13)$$

$$\mathbf{C}(z) \triangleq \begin{bmatrix} C_{1,1}(z) & C_{1,2}(z) \\ C_{2,1}(z) & C_{2,2}(z) \end{bmatrix} \quad \mathbf{g}(z) \triangleq \begin{bmatrix} 2H_0^p(z) \\ -2H_0^p(-z) \end{bmatrix} \quad (14)$$

We then have

$$E(z) = \frac{1}{2}\mathbf{g}^T(z)\left[\mathbf{H}(z)\mathbf{S}(z) - \mathbf{C}(z^2)\mathbf{H}(z)\right]\mathbf{x}(z) \quad (15)$$

We take $C_{1,2}(z) = 0$, $C_{2,1}(z) = 0$ since cross-channel predictors are not used. The aliasing occurs around $\theta = \frac{\pi}{2}$. Therefore, we evaluate (15) at $\theta = \frac{\pi}{2}$, use Theorem 1 and obtain

$$E(\tfrac{\pi}{2}) = -\left[H_0^{2p}(\tfrac{\pi}{2})C_{1,1}(\pi) - H_1^{2p}(\tfrac{\pi}{2})C_{2,2}(\pi)\right]X(\tfrac{\pi}{2}) - H_0^{2p}(\tfrac{\pi}{2})H_1^{2p}(\tfrac{\pi}{2})\left[C_{1,1}(\pi) - C_{2,2}(\pi)\right]X(-\tfrac{\pi}{2}) \quad (16)$$

Clearly, if

$$C_{1,1}(\pi) = C_{2,2}(\pi) \quad (17)$$

we have $E(\frac{\pi}{2}) = 0$. Therefore, the *continuity constraint* guarantees that the component of the residual echo signal at $\theta = \frac{\pi}{2}$ is zero. Since the notch due to the CPS-IIR filter bank has a non-zero transition-band, the spectral components around $\theta = \frac{\pi}{2}$ will also be attenuated.

5. NLMS ALGORITHM WITH CONTINUITY CONSTRAINTS

The necessity to use continuity constraints requires the modification of the adaptive algorithms that update $C_{1,1}$ and $C_{2,2}$. Consider binary-tree decomposition into four subbands where the transversal adaptive filters in each subband are respectively denoted by $W_i, i = 1,2,3,4$. The continuity constraints across the subband edges are at the reduced rate (i.e. at $\theta = 0$ and $\theta = \pi$) and in terms of W_i they are given by

$$\mathcal{Z}_1^T W_1(k) = \mathcal{Z}_2^T W_2(k) \quad (18)$$

$$\mathcal{K}_2^T W_2(k) = \mathcal{K}_4^T W_4(k) \quad (19)$$

$$\mathcal{Z}_3^T W_3(k) = \mathcal{Z}_4^T W_4(k) \quad (20)$$

$$\mathcal{Z}_i^T = [1\ 1\ 1\ 1\ \ldots]_{1\times L_i},\ \mathcal{K}_i^T = [1\ {-1}\ 1\ {-1}\ \ldots]_{1\times L_i} \quad (21)$$

where $L_i, i = 1,2,3,4$ are the number of adaptive coefficients in each subband. The above constraints are mild since the adaptive coefficients are not forced only to be spectrally continuous across the subbands.

In [5], it is shown that when (18)-(20) are imposed on the NLMS algorithms running in four subbands, the update equations of the four-band CC-NLMS algorithm are

$$W_1(k) = W_1(k-1) + \frac{\mu_1 \underline{e}_1(k)}{\|X_1(k)\|_2^2}X_1(k) - \lambda_1^* \mathcal{Z}_1 \quad (22)$$

$$W_2(k) = W_2(k-1) + \frac{\mu_2 \underline{e}_2(k)}{\|X_2(k)\|_2^2}X_2(k) + \lambda_1^* \mathcal{Z}_2 - \lambda_2^* \mathcal{K}_2 \quad (23)$$

$$W_3(k) = W_3(k-1) + \frac{\mu_3 \underline{e}_3(k)}{\|X_3(k)\|_2^2}X_3(k) - \lambda_3^* \mathcal{Z}_3 \quad (24)$$

$$W_4(k) = W_4(k-1) + \frac{\mu_4 \underline{e}_4(k)}{\|X_4(k)\|_2^2}X_4(k) + \lambda_2^* \mathcal{K}_4 + \lambda_3^* \mathcal{Z}_4 \quad (25)$$

where $\underline{e}_i(k) = m_i(k) - y_i(k)$ and λ_1^*, λ_2^*, λ_3^* are the optimal Lagrange multipliers given by

$$\lambda_1^* = \frac{1}{L_1 + L_2}\left(\frac{\mu_1 \underline{e}_1(k)}{\|X_1(k)\|_2^2}\mathcal{Z}_1^T X_1(k) - \frac{\mu_2 \underline{e}_2(k)}{\|X_2(k)\|_2^2}\mathcal{Z}_2^T X_2(k)\right) \quad (26)$$

$$\lambda_2^* = \frac{1}{L_2 + L_4}\left(\frac{\mu_2 \underline{e}_2(k)}{\|X_2(k)\|_2^2}\mathcal{K}_2^T X_2(k) - \frac{\mu_4 \underline{e}_4(k)}{\|X_4(k)\|_2^2}\mathcal{K}_4^T X_4(k)\right) \quad (27)$$

$$\lambda_3^* = \frac{1}{L_3 + L_4}\left(\frac{\mu_3 \underline{e}_3(k)}{\|X_3(k)\|_2^2}\mathcal{Z}_3^T X_3(k) - \frac{\mu_4 \underline{e}_4(k)}{\|X_4(k)\|_2^2}\mathcal{Z}_4^T X_4(k)\right) \quad (28)$$

provided that L_2 and L_4 are chosen as even numbers. Note that, a safety constant, $\nu_i > 0$, can be added to each normalisation factor, $\|X_i(k)\|_2^2$, and this does not violate the continuity constraints.

The terms $\frac{\mu_i}{\|X_i(k)\|_2^2}\underline{e}_i(k)X_i(k)$ are already computed for the update equations in (22)-(25). Therefore, no extra multiplication operations are required in the proposed algorithm. If $L_i = 2^q$, then the divisions $\frac{1}{L_i+L_j}$ in (26)-(28) correspond to arithmetic left shift operations. However, further addition/subtraction operations are required which is given by $\frac{1}{4}(9 + 2\sum_{i=1}^{4} L_i)$ at the full-rate.

6. SIMULATIONS

Two experiments are conducted with artificial and real signals in order to evaluate the performance of the proposed AEC system. The level of echo cancellation is measured by using the Segmental Echo Return Loss Enhancement (S-ERLE), which is defined as

$$\text{S-ERLE}(i) \triangleq 10\log_{10}\left(\frac{\sum_{k=(i-1)S}^{iS-1} m^2(k)}{\sum_{k=(i-1)S}^{iS-1} e^2(k)}\right), \quad i = 1,2,\ldots \quad (29)$$

where S is the window size, $m(k)$ is the microphone signal, and $e(k)$ is the corresponding full-band residual echo signal. The Time of Initial Convergence (TIC) is also measured as the time elapses until S-ERLE(i) = 10dB.

In both experiments, four techniques are used for echo cancellation. Firstly, the prototype PR-FIR filter in Fig. 1 is used in the analysis and synthesis banks. The NLMS algorithm is used in each subband. Secondly, PS-IIR filter banks are used rather than PR-FIR filter banks. Thirdly, the previous technique is used with the DNFs [4]. Finally, the proposed CPS-IIR filter banks are used with the four-band CC-NLMS algorithm.

Experiment 1: The loudspeaker signal is chosen as zero-mean and white with unity average power. A 256-tap echo path impulse response is used which is measured in a car. The number of subbands is 4 and the step-sizes in each subband are chosen as 0.5. Each subband adaptive filter has 64 coefficients. The residual echo signals are averaged over 50 Monte-Carlo trials. The results for this experiment are tabulated in Table 2.

The amplitude spectra of the residual echo signals after convergence are illustrated in Fig. 2 - 3. The notches for the proposed CPS-IIR + CC-NLMS technique are clearly visible.

Experiment 2: Experiments are conducted with female and male speech signals recorded in a car with 8KHz sampling frequency. The step-sizes and the lengths of the adaptive filters are the same as in the previous experiment. The corresponding results are presented in Table 3, where Max(S-ERLE), Mean(S-ERLE), and TIC-10dB are provided

Technique	Max (S-ERLE)	Mean (S-ERLE)
PR-FIR,NLMS	10.6 dB	9.8 dB
PS-IIR,NLMS	15.3 dB	14.0 dB
PS-IIR,DNF ,NLMS	26.4 dB	25.8 dB
CPS-IIR ,CC-NLMS	23.0 dB	22.1 dB

Table 2: Experimental results with white input signal. The number of subbands is 4.

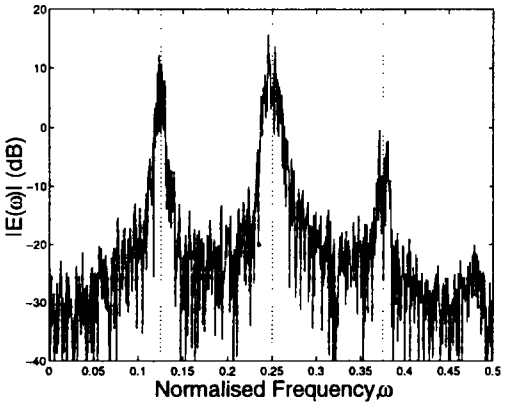

Figure 2: Amplitude spectrum of the residual echo for the PS-IIR + NLMS technique, $\omega = \frac{\theta}{2\pi}$.

with $S = 250$ in (29). The results indicate that the performance of the proposed CPS-IIR + CC-NLMS technique is similar to the performance of the PS-IIR + DNF + NLMS technique. The PR-FIR + NLMS technique yields the lowest ERLE performance and the slowest convergence behaviour.

Technique	Max (S-ERLE)	Mean (S-ERLE)	TIC-10dB
PR-FIR,NLMS	20.5 dB	11.3 dB	112.0 msec.
PS-IIR,NLMS	21.1 dB	11.9 dB	80.0 msec.
PS-IIR,DNF ,NLMS	22.3 dB	13.5 dB	80.0 msec.
CPS-IIR ,CC-NLMS	22.1 dB	13.0 dB	80.0 msec.

Table 3: Experimental results with real speech recordings. The number of subbands is 4.

The results in both experiments clearly demonstrate the attenuation of the aliased components around the subband edges.

7. CONCLUSIONS

Power Symmetric IIR filters are used in cascade form and a new analysis and synthesis banks are proposed which can be implemented as polyphase networks. It is shown that when the number of cascades is even, there is a notch at the subband division frequency at the output of the analysis bank

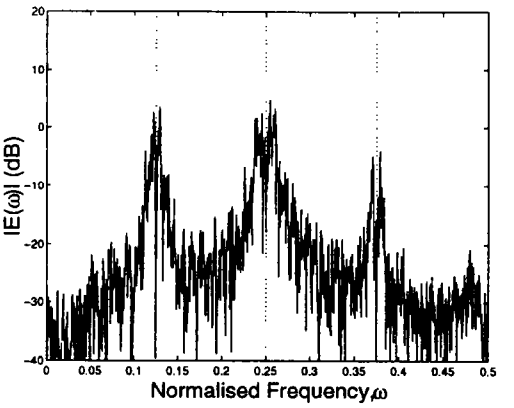

Figure 3: Amplitude spectrum of the residual echo for the CPS-IIR + CC-NLMS technique, $\omega = \frac{\theta}{2\pi}$.

followed by the synthesis bank. It is also shown that adaptive filters in neighbouring subbands must be coupled via continuity constraints. The NLMS algorithm is therefore modified and the CC-NLMS algorithm is proposed. The experimental results validate the anticipated attenuation of the aliasing around the subband division frequencies.

8. REFERENCES

[1] A. Gilloire and M. Vetterli. Adaptive filtering in subbands with critical sampling:Analysis, experiments and application to acoustic echo cancellation. *IEEE Trans. Sig. Proc.*, 40(8):1862–1875, Aug. 1992.

[2] W. Kellermann. Analysis and design of multirate systems for cancellation of acoustical echoes. In *ICASSP-88*, pages 2570–2573, New York, NY, USA, Apr. 1988.

[3] O. Tanrikulu, B. Baykal, A. G. Constantinides, and J. A. Chambers. Residual signal in sub-band acoustic echo cancellers. In *EUSIPCO-96*, pages 21–24, Trieste, Italy, Sept. 1996.

[4] O. Tanrikulu, B. Baykal, A. G. Constantinides, and J. A. Chambers. Residual signal in critically sampled subband acoustic echo cancellers based on IIR and FIR filter banks. *IEEE Trans. Sig. Proc.*, Apr. 1997.

[5] O. Tanrikulu and A. G. Constantinides. Cascaded power symmetric IIR filter banks in subband adaptive filtering with application to acoustic echo cancellation. *Submitted to IEEE Trans. Sig. Proc.*, Jan. 1997.

[6] P. P. Vaidyanathan. *Multi-rate Systems and Filter Banks*. Englewood Cliffs, NJ: Prentice-Hall, 1993.

[7] R. A. Valenzuela and A. G. Constantinides. Digital signal processing schemes for efficient interpolation and decimation. *IEE Proc.*, 130(6):225–235, Dec. 1983.